Accuracy Improvement for Indoor Positioning Using Decawave on ESP32 UWB Pro with Display and Regression

Gita Indah Hapsari [1], Rendy Munadi [2*], Bayu Erfianto [3], Indrarini Dyah Irawati [4]
[1, 2, 3, 4] Department of Informatics, Telkom University, Bandung, Jawa Barat, Indonesia
Email: [1] gitaindahhapsari@telkomuniversity.ac.id, [2] rendymunadi@telkomuniversity.ac.id, [3] erfianto@telkomuniversity.ac.id,
[4] indrarini@telkomuniversity.ac.id
*Corresponding Author

Abstract—In UWB-based indoor positioning, it is important to observe the ranging performance of the UWB module to prevent positioning errors. Ranging is the initial process in computing positioning. This research aims to observe the ranging accuracy and precision of the ESP32 UWB Pro with a Display module and analyze its performance in indoor positioning using TDoA and Trilateration. The ranging method was held using the SS-TWR which is the basic ranging used generally in UWB. ESP32 Pro is a module consisting of ESP32 and OLED display which is integrated with Decawave DW 1000. Analysis of 6750 ranging error data is carried out to determine the appropriate method to increase accuracy. The convergence of error ranges that occur leads to the use of regression as an error mitigation method for Decawave on the ESP32 UWB Pro with Display module. Increasing the accuracy of ranging regression can reduce the error from MAE of 79.98cm to only 5.05cm. It's applied to positioning to obtain the accuracy and precision performance of the TDoA and Trilateration positioning. The resulting MAE values are 7.47cm for X and 10.49cm for Y in TDoA Positioning. Meanwhile, in Trilateration, the MAE was 8.15cm for X and 8.47cm for Y. Our findings indicate that an increase in ranging accuracy with regression had an impact on positioning accuracy. However, the spread of error positioning shows that it's still weak in precision.

Keywords—*Accuracy Improvement; Ranging Error; ESP32 UWB Pro with Display; Regression; Indoor Positioning.*

I. INTRODUCTION

Indoor Positioning is a process for estimating the position of a device in the form of a stationary object or a moving object indoors. The tag installed on the device emits a signal or sends a message to be captured by a group of anchors to estimate the tag's position. An anchor is a device that is placed in a certain position and its position is known. The anchor is used as a reference to estimate the tag position. In indoor positioning, GPS cannot be used to estimate positioning because there is a reduction in the power of the GPS signal due to the complexity of the indoor environment, so the GPS becomes inaccurate [1].

Position estimation information is needed for various implementations. Many IoT-based applications currently use position information for tracking [2][3][4][5][6] and navigation [7]. The need for position information also occurs in the industry[8], industrial robot tracking [9], warehouse [10], and positioning systems in static and mobile cases in the industry [11]. Indoor positioning also applies in underground mining [12][13].

Various sensors were introduced by researchers to carry out positioning [14], including using signals such as RF [15][16], Bluetooth [17][18][19], RFID [20][21][22], WiFi [23][24], and UWB [25][26][95]. The use of other sensors such as the Inertial Measurement Unit (IMU) [12][27][28], camera [29][30], and Visible Light Positioning (VLP) [31][32][33] is also proposed by researchers for positioning indoors.

The choice of UWB signal in this research is supported by promising research trend data on indoor positioning and mobile anchors [34]. UWB is a form of radio signal used for positioning which is famous for its accuracy. Fig. 1 is a comparison of the parameters of each signal based on accuracy, noise resistance, cost, power consumption, and coverage [35][7][36]. As shown in Fig. 1, UWB has advantages in almost all parameters, so UWB is very reliable for indoor positioning. However, this accuracy problem is still a challenge for researchers. The factor causing position error is the complex measurement environment because there are many obstacles.
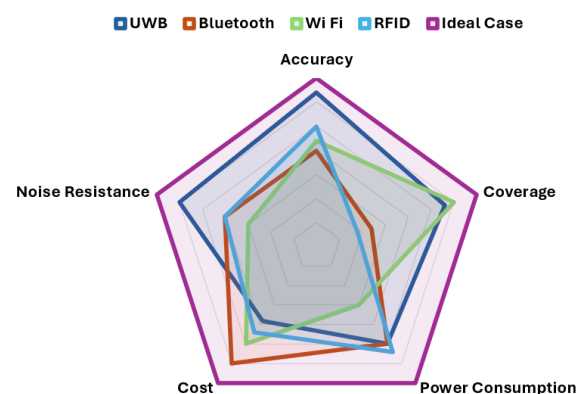

Fig. 1. UWB Performance among other signals

UWB is a signal for positioning that has a very wide bandwidth ranging from 3.1 GHz to 10.6 GHz with a power level below 41.3 dBm/MHz based on ITU-R SM.1757-0 [37]. The wide bandwidth means that UWB is also reliable against narrowband signal interference [38]. Based on the paper [35], UWB is a signal with accuracy ranging from

meters to centimeters for use in indoor positioning. Even though UWB has high accuracy, the complexity of the room or Non-Line of Sight (NLOS) due to obstacles can cause signal propagation to be disrupted [35][39][40]. Attenuation caused by obstacles such as reflection and refraction can cause a reduction in positioning accuracy. Various methods for preventing errors in complex environments, either using machine learning or statistics, continue to observe position measurement results in the LOS environment. It is important to observe the performance of the indoor positioning system in the LOS environment before used in the NLOS environment. The comparison of error performance in LOS and NLOS environments can determine the next method that will be used to mitigate ranging errors in NLOS conditions.

Ranging is a process of estimating the distance between the anchor and the tag before calculating the position estimation. The estimated ranging value is then used to calculate the estimated position of the tag relative to the anchors. Ranging using UWB signals is carried out on a time-based basis, namely Time of Flight (ToF) [41][42] or Two Way Ranging (TWR) [43][44][45]. As shown in Fig. 2, Ranging is the initial process for measuring the distance between the anchor and tag which can produce errors. Errors that occur are then reduced to improve accuracy and prevent errors in positioning. The results of the mitigated ranging are then implemented in the positioning process to produce the X and Y positions of the tag using several approaches such as TDoA, Trilateration, or Multilateration [46].
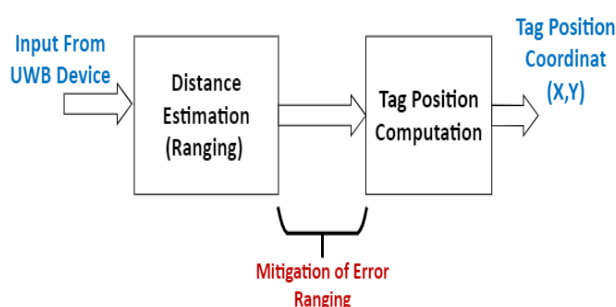

Fig. 2. Positioning process

Accuracy in ranging values greatly influences the accuracy of positioning estimation results [47][48]. Errors that occur in the ranging process can cause larger errors in positioning because ranging is used to compute the positioning in geometry. Positioning errors can have a big impact, especially in implementation cases that require high accuracy such as automated industrial robots in the form of drones, asset tracking, and automatic control systems in vehicles.

Unfortunately, in some cases, there are still ranging errors that cause higher errors in the positioning process due to the performance of the UWB module. There are different performance parameters between each kind of UWB module, especially in accuracy and precision. Antonio Ramon et al [49] observed 3 UWB modules, namely Ubisense, Be Spoon, and Decawave. A comparison of ranging estimation precision is carried out to compare the performance of the three modules in an experiment and test them in the same environment. From the experimental results, different ranging errors precision were produced between each module. Likewise, Tommaso et al compared the performance of the DW1000 and DW3000. The research results show that both have the same precision for ranges above 1 m, but the DW3000 has better precision performance for shorter distances [50]. This shows that each module has a different performance, and it is important to observe the module performance to be used for positioning. If an error occurs in ranging, accuracy improvement is needed to reduce errors in the ranging process [51].

Several studies were proposed by researchers to increase the accuracy of the ranging process as detailed in Table I. Barbara et al [49], in their research, increased the accuracy of the Pozyx and Decawave modules by applying the filtering method. This method is implemented in static and dynamic positioning. Static positioning results in a reduction in error to 32 cm for the Pozyx module and 25 cm for the DecaWave Module. Meanwhile, Antonio et.al [51] improved the accuracy of the Decawave UWB MDEK1001 module by applying the Gaining Access to Multiple Range method. This method succeeded in increasing positioning accuracy to produce an error of 0.2m.

In other research, Sidorenko et al [52] proposed an error correction ranging method for TWR using the DecaWave DW1000 module. This method is quite reliable for TDoA positioning and produces precision of up to 0.221m. However, the resulting ranging error is still relatively high at the decimeter level. The method proposed in this paper is regression using DW1000.DW1000 is a decawave module that has the best accuracy and precision performance between Ubisense and Be Spoon. Therefore, this research uses ESP 32 UWB pro with display which contains a DW 1000 Decawave chip. This regression method succeeded in reducing the ranging error to 5.05 cm for 1-10 meters.

TABLE I.　Recent Study in Improving Accuracy UWB Module and Proposed Method

Paper	Improvement Accuracy Method	UWB Module	Error Ranging Result	Implementation
Barbara et al [49]	Median Filter, Arma Filter, Kalman Filter	Pozyx and Decawave	Not mention	Static and Dynamic Triangulation. Pozyx 32 cm Decawave 25 cm
Antonio et al [51]	Gaining Access to Multiple Range	MDEK1001	Average error 2.3 cm	Multilateration 0.2 m
Sidorenko et al [52]	error corection ranging twr	decawave DW1000	Not mention	TDoA MultiLateration
Proposed method	Regression	Decawave DW1000	MAE 5.05 cm	Positioning TDoA and trilateration 0.08m-0.1m

In this research, an analysis was carried out on the ranging error and precision produced by the ESP 32 DW1000 pro with display module. Accuracy improvement using regression is carried out to reduce the resulting ranging error and then applied to positioning using the TDoA and Trilateration methods to determine the performance of positioning accuracy and precision. Based on the results of the error analysis, regression was decided to be used to mitigate ranging errors.

The results of measuring estimated ranging against real ranging are made into a regression model to be embedded in the ranging process for positioning. The ranging results from regression mitigation are then used in positioning to analyze the precision of the positioning estimation results after ranging mitigation.

The objectives of this research are (i) to increase accuracy by applying a regression method based on error ranging analysis produced by the ESP32 UWB Pro with display module and (ii) to implement ranging regression results in indoor positioning using TDoA and Trilateration and observing the performance of accuracy and precision.

The contributions of this research are:

1. Propose a ranging error improvement accuracy method for the ESP32 UWB Pro with a display module using a regression approach at the centimeter level.

2. Provide an improvement of accuracy and precision indoor positioning using TDoA and Trilateration using regression ranging method.

II. MATERIAL AND METHOD

A. ESP32 UWB Pro with Display Module

The module used in this research is the UWB DW 1000 Pro with display. This module is an integration between ESP 32, DW1000, and Oled Display. This module has 4MB Flash and 8MB with a physical appearance as in Fig. 3. This module is produced by Makerfabs and is equipped with a Lippo battery charger and connector so that this module can work separately using a PSRAM battery [53].

As shown in Fig. 3, this module uses the DW1000 which is a single-chip CMOS radio transceiver IC with the IEEE 802.15.4-2011 ultra-wideband (UWB) standard. The DW1000 works on channels 5 and 6 of the UWB bandwidth. The datasheet claims that the DW1000 has a ranging accuracy of around 10 cm using ToF [54][55]and TWR [56][57].
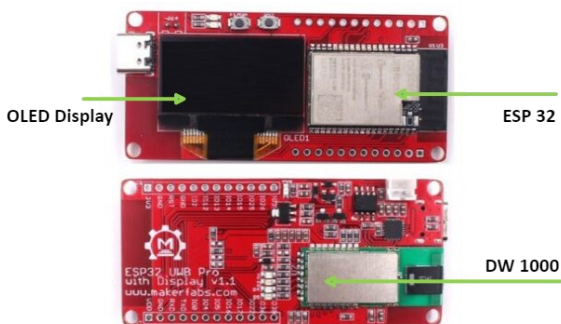

Fig. 3. ESP32 UWB Pro with display module

B. Method

As shown in Fig. 4, the research method begins with ranging measurements using SS-TWR. Ranging measurements are carried out at each meter for actual distances ranging from 1m to 15 meters. Ranging measurements were carried out for 50 seconds and produced estimated ranging data of around 450 data in each meter. Next, the Mean Absolute Error (MAE) and Mean Squared Error (MSE) values are calculated to determine accuracy. The error between estimated ranging and actual ranging is analyzed using the normal distribution and Q-Q Plot to analyze whether the error is systematic or random. The resulting systematic error determines the use of regression as a method to increase ranging accuracy in the next step. The new ranging resulting from regression is then implemented in indoor positioning using TDoA and Trilateration. Performance analysis of accuracy and precision is carried out on ranging and positioning results.

1) Ranging Measurement

The ranging process is carried out using the Two-Way Ranging (TWR) technique to estimate the distance between the anchor and the tag without time synchronization [58][59]. SS-TWR (Single Side-TWR) is a ranging technique used in this experiment as shown in Fig. 4.

Ranging is a process of calculating the estimated distance between the anchor and the tag. TWR is a time-based ranging technique that computes distance by measuring the signal travel time from anchor to tag or vice versa. The TWR technique is shown in Fig. 5. If the message is sent at time τ_{ATX} from device 1 and arrives at device 2 at time τ_{BRX}, then the signal propagation time from device A to device B is Ttof, then the distance between device 1 and device 2 can be calculated using the formula (1).

$$r = cxT_{tof} \qquad (1)$$

r is the distance between device A and device B (meter), c is the velocity of light 3×10^8 m∕s, and T_{tof} is the time of signal propagation from device A to device B (second).
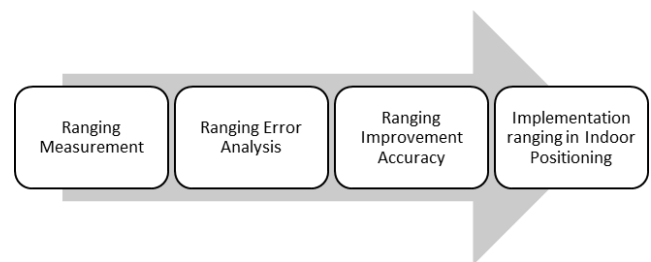

Fig. 4. Experiment and Analysis

Two Way Ranging (TWR) is one way to eliminate clock synchronization between devices. There are 4 types of TWR techniques including Single-Side TWR (SS-TWR), Symmetric Double side TWR (DS-TWR), and Asymmetric Double TWR (ADS-TWR) [43], [44], [45]. SS-TWR can be seen in Fig. 5 where the signal is sent from device A at time τ_{ATX} and arrives at device 2 at time τ_{BRX}. Device B sends a reply signal to device A. This is done to eliminate the time synchronization process between device A and device B.

Device B takes time to send a reply signal during t (reply B). Device B sends a reply signal at time t_{BTX} and is received at device A at time t_{ARX}. The signal propagation time from device A to device B and then back to device A is t_{roundA} which can be calculated based on formula (2.2). t_{roundA} can also be calculated with $t_{roundA}=t_{ARX}-t_{ATX}$. From formula (2), T_{tof} can be calculated using formula (3) so that the distance between devices can be calculated using formula (1).

$$t_{round\ A} = 2.T_{tof} + t_{reply\ B} \tag{2}$$

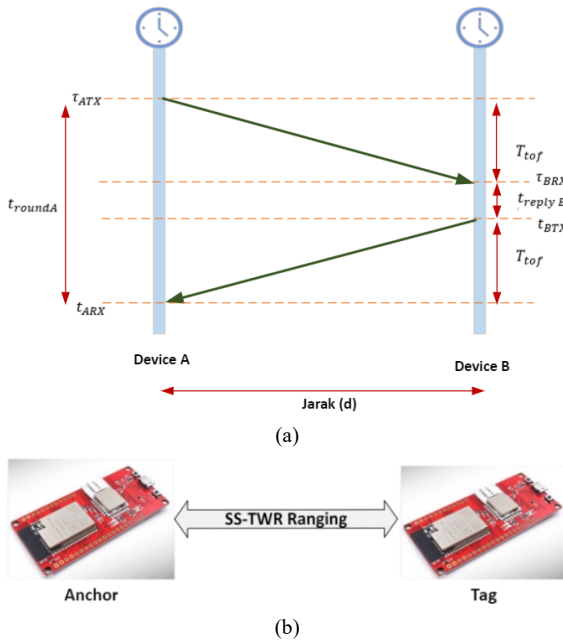$$T_{tof} = \frac{1}{2}(\ t_{round\ A} - t_{reply\ B)} \tag{3}$$

(a)

(b)

Fig. 5. Ranging Process: a) SS-TWR ranging Process and b) Ranging Experiment using UWB Module

The ranging experiment is shown in Fig. 6 using 2 UWB modules by measuring the distance between anchors and tags at certain distance intervals ranging from 1m to 15 m. The results of the ranging error analysis confirm that the regression method can be used to mitigate ranging errors. The ranging measurement environment is shown in Fig. 6. Ranging measurements are carried out in an LOS environment without any obstacles between the anchor and tag with the antenna direction facing each other.
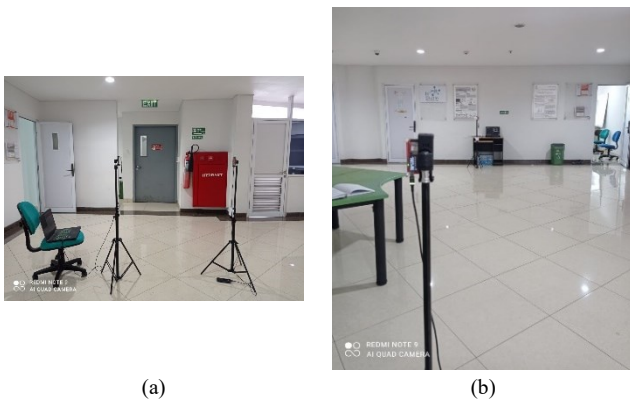

(a)   (b)

Fig. 6. Ranging experiment: (a) 1m (b) 15m

2) Ranging Error Analysis

Calculation of accuracy from ranging estimates to actual distance is carried out using MAE with the formulas shown in formulas (4) and (5). This accuracy value will then be compared with the accuracy of the ranging estimate after increasing the accuracy using regression.

$$\varepsilon = \frac{\sum_{i=1}^{n} |\hat{y}_i - y_i|}{n} \tag{4}$$

Determining the type of error and precision are determined through error analysis using a normal distribution based on standard deviation or STD from the normal distribution graph. Precision error is determined by calculating the standard error using formula (5). Variable n is the total number of observations, and σ is the standard deviation or standard error which is calculated from the RMS value and the mean of ϑ.

$$\sigma^2 = \frac{1}{n}\sum(\vartheta_i - \hat{\vartheta})^2 \tag{5}$$

The ranging error dataset was tested for normality based on skewness and kurtosis introduced by D'Agostino et al (1990). Kurtosis means the curvature or degree of taper of a distribution. If the P value is greater than 0.05 then the data is normally distributed[ ]. The results of this normality test are one of the considerations why regression was chosen as a method for increasing ranging accuracy. (D agostinos formula).

One approach to increasing accuracy is to apply an error correction model. Regression is an error correction model that is usually used to handle linear errors and convergent errors. Linearity can be proven using a Q-Q Plot or normal Probability Plot. The Q-Q (quantile-quantile) plot and the normal probability plot are essentially the same type of plot. They both serve as graphical tools for assessing whether a dataset follows a normal distribution or some other theoretical distribution. Q-Q plot is a quantile graph that provides an overview of a normally distributed data set formed from observation values with their standard normal quantile values. If the points are obtained from a straight line, it can be concluded that the data tends to be normally distributed. QQ plot is one of the graphs used to guarantee that an estimation model is a regression [60].

3) Ranging Improvement Accuracy

The normality obtained from ranging error analysis strengthens the determination of regression as a method to reduce error values and increase accuracy in ranging. The regression formula is shown in formula (6).

$$Y = \alpha + \beta_1 X_1 + \cdots + \beta_k X_k + \varepsilon \tag{6}$$

The ranging results after regression are then applied to the ESP32 UWB Pro with a display module. Comparisons were made to range estimates before and after improving accuracy. To validate the ranging mitigation results, the ranging results after mitigation with higher accuracy are applied to positioning using 2 approaches, namely TDoA and Trilateration. The positioning results from both methods are analyzed and compared based on accuracy and precision.

Algorithm 1 : Positioning with Ranging Regression

1. **Define the coordinat anchor for TDoA and Trilateration**
   - **TDoA**
   $$\forall_1 = (1.8m, 0.8m)$$
   $$\forall_2 = (7.8m, 0.8m)$$
   - **Trilateration**
   $$\forall_1 = (1.8m, 0.8m)$$
   $$\forall_2 = (7.8m, 0.8m)$$
   $$\forall_3 = (4.8m, 10.8m)$$

2. **Define distance of anchor TDoA:**
   $$d = 6m$$

3. **Measure and calculate ranging from tag to each anchor as r :**
   $$r_n = cxT_{tof}$$

4. **Calculate ranging regression as $\hat{r}$:**
   $$\hat{r}_n = 0.981 - 0.6621r$$

5. **Calculate tag position $X_s \, dan \, Y_s$ using :**
   - **TDoA**
   $$X_s = b.\cos\alpha = \hat{r}_1 * (\hat{r}_1^2 + d^2 - \hat{r}_2^2/2 * \hat{r}_1 * d)$$
   $$Y_s = b.\sin\alpha = \hat{r}_1 * \sqrt{1 - \cos^2\alpha} = y_1 * \sqrt{1 - (\hat{r}_1^2 + d^2 - \hat{r}_2^2/2 * \hat{r}_1 * d)}$$
   - **Trilateration**
   $$2\begin{bmatrix} Xc - Xa & Yc - Ya \\ Xc - Xb & Yc - Yb \end{bmatrix}\begin{bmatrix} Xs \\ Ys \end{bmatrix} = \begin{bmatrix} (\hat{r}_1^2 - \hat{r}_3^2) - (xa^2 - xc^2) - (ya^2 - yc^2) \\ (\hat{r}_2^2 - \hat{r}_3^2) - (xb^2 - xc^2) - (yc^2 - yc^2) \end{bmatrix}$$

---

4) Implementation Ranging in Indoor Positioning

Ranging with improved accuracy is then implemented in indoor positioning to observe its accuracy and precision performance. Positioning is implemented using TDoA and Trilateration techniques. TDoA uses 2 anchors to estimate the position of the tag [61][62][63][64]. TDoA relies on calculating the angle and distance between the two anchors as shown in Fig. 7. The S Tag position calculation can be calculated using formulas (7) and (8). Meanwhile, Trilateration uses 3 anchors to calculate the tag position [65] as shown in Fig. 8. The position of Tag S is determined based on the ranging value between anchors A, B, C and Tag S. The formula for calculating the position of tag S is shown in equation (9).

$$X_s = b.\cos\alpha \quad (8)$$

$$Y_s = b.\sin\alpha \quad (9)$$

$$2\begin{bmatrix} Xc - Xa & Yc - Ya \\ Xc - Xb & Yc - Yb \end{bmatrix}\begin{bmatrix} Xs \\ Ys \end{bmatrix} = \begin{bmatrix} (\hat{r}_1^2 - \hat{r}_3^2) - (xa^2 - xc^2) - (ya^2 - yc^2) \\ (\hat{r}_2^2 - \hat{r}_3^2) - (xb^2 - xc^2) - (yc^2 - yc^2) \end{bmatrix} \quad (10)$$
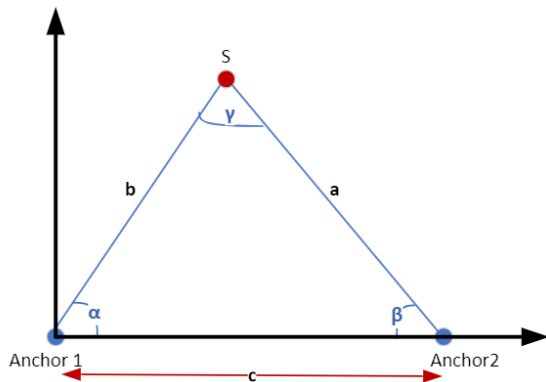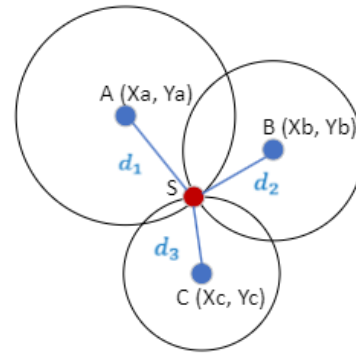
Fig. 7. TDoA positioning

Fig. 8. Trilateration positioning

III.   RESULT AND DISCUSSION

A. Error Ranging Analysis and Regression

Ranging error analysis was carried out on the error values resulting from anchor and tag distance measurements using the ESP32 UWB pro with Display module. Ranging measurements start from 1 m to 15 m with an increase in distance of 1 meter for each measurement. Ranging measurements were carried out for 50 seconds and produced estimated ranging data of around 6750 data in each meter.

The actual position is measured using a SNDWAY laser meter which has a tolerance of 2mm based on the datasheet so ground truth position will be ±2mm. Fig. 9 shows an analysis error ranging graph sample of 15 m which consist of 450 data. The average (mean) of the error-ranging data is 0.8174 m and the standard deviation is 0.0179 m. The boxplot in Fig. 9(b) shows that the average value of 0.8174 m is still around the median of 0.82 so the skewness is slightly towards the left. The boxplot also shows the lowest and highest margin values for ranging errors, namely 0.78 and 0.87. There are 2 outliers in the boxplot, but these are

ignored compared to the total number of measurement data which reaches 450 data.

Normality testing is carried out to determine the distribution of ranging errors that occur. Normality testing is carried out graphically using the Normal Probability Plot graphic plotting as in Fig. 9(c). Based on this figure, the error values follow the confidence line and almost all of them are plotted in the confidence interval area. This shows that the error ranging data is included in the normal distribution.
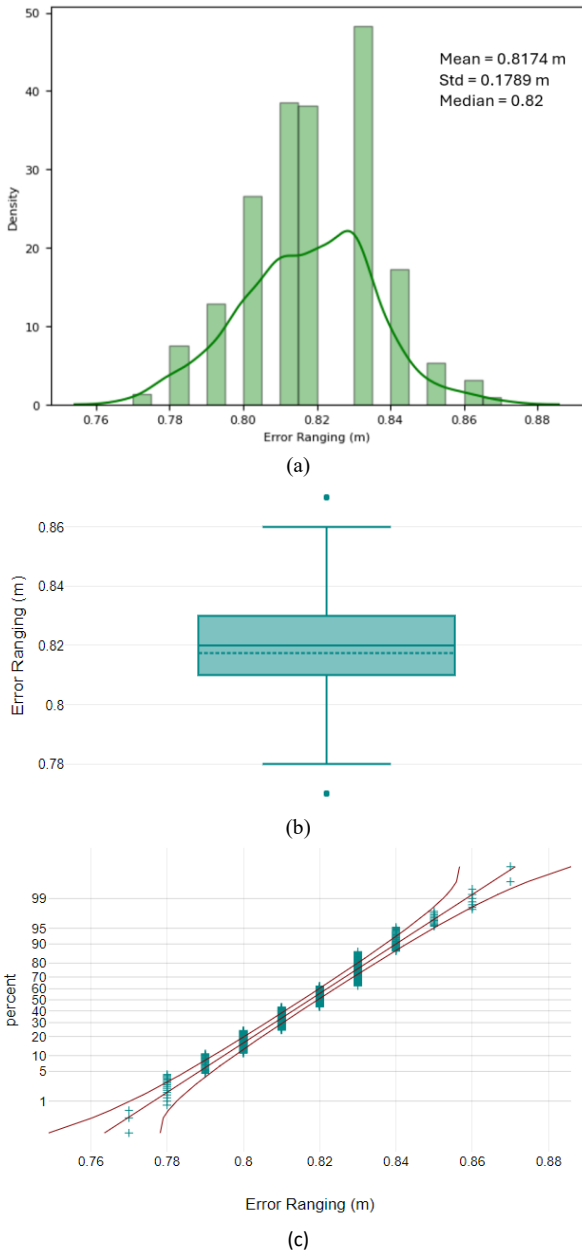

(a)

(b)

(c)

Fig. 9. Error Ranging Analysis Sample of 15 m: (a) The Histogram of distribution, (b) Boxplot, and (c) Normal Probability Plot

Normality was also tested based on skewness and kurtosis to strengthen the proof of normality in the error-ranging data. The p-value produced using D'agostinos is 0.69. This value is greater than 0.05 so that the ranging error data falls into a normal distribution. The results of the Normal Probability Plot and P-value plotting show linear

data and lead to the use of regression as a method of increasing accuracy. There are several outliers in each measurement section per meter in the Normal Probability plot, but they still have a pattern that is in the same direction as the confident line on the graph so that the plot results still lead to linearity.

The regression equation is built from the results of the average ranging estimated value for each meter of actual distance. The estimated average ranging value per meter is plotted against the actual distance value to produce a blue graph as shown in Fig. 10. This graph has a parallel relationship with the red ideal graph of ranging measurements x=y. This strengthens the basis for choosing a regression approach to increase ranging error. The resulting regression equation is shown in Equation (11).

$$y = 0.981 - 0.6621x \qquad (11)$$

The regression equation is then embedded in the ranging program on ESP32 UWB Pro with Display and measurements are carried out again with the same scenario to see the results of the improvement accuracy after the regression is applied. Measurements of ranging were carried out again to prove the reduction in error after regression.
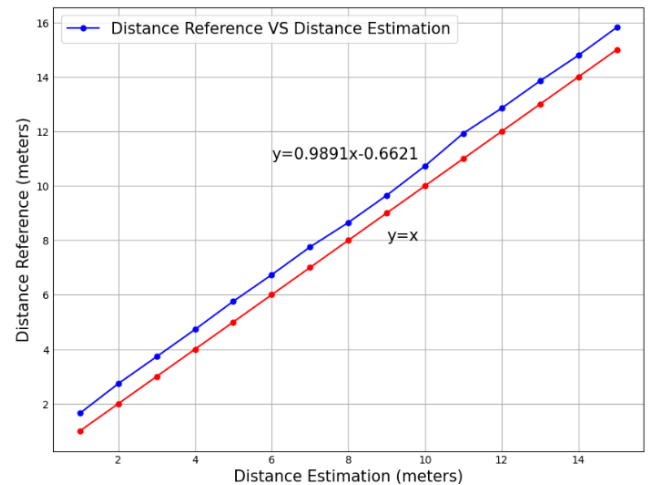

Fig. 10. Ranging regression

Ranging measurements after regression are carried out with the same scenario as before. For each meter of measurement, an average ranging estimate is calculated. This value is plotted on a red graph and compared directly with the blue y=x graph in Fig. 11. The two graphs coincide with each other and through the coefficient of determination test the resulting R2 value is 0.9999. This shows that almost all estimated ranging values can represent actual ranging values.

MAE ranging calculations are carried out on each meter of ranging measurements before and after regression. The MAE value from ranging before regression produced a high value reaching 75.78 cm. Meanwhile, after regression, the MAE value was only 5.30 cm. This shows that accuracy has increased quite significantly from the decimeter to centimeter level after regression implemented in ranging. The comparison of MAE values is described in Fig. 12. This shows that error improvement using regression is quite

effective in reducing errors on the ESP32 UWB PRO with display module with an increase in accuracy of around 70 cm.
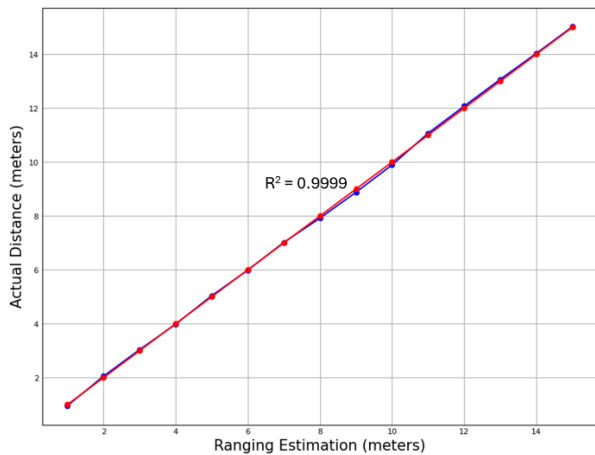

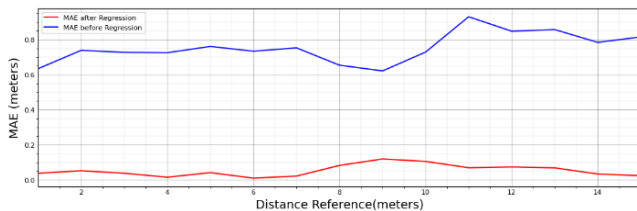Fig. 11. The result of ranging estimation after regression

Fig. 12. Mean Absolute Error Before and After Mitigation

B. Positioning Performance with Ranging Mitigation Using TDoA and Trilateration

Ranging with better accuracy is then implemented in indoor positioning using TDoA and Trilateration techniques.

TDoA is a positioning method that uses only 2 anchors to position a tag. Testing was carried out in a meeting room with an area of 8.4m×13.8m as shown in Fig. 13 and Fig. 14. Anchors are placed at the front of the room with a distance between anchors of 6 meters. Tags are positioned according to certain positions whose coordinates have been measured on ground truth. Ground truth coordinate measurements were carried out manually using a laser meter and measuring tape.

In TDoA positioning, 2 anchors are installed parallel to 6 meters at coordinate positions (1.8m, 0.8m) and (7.8m, 0.8m) as shown in Fig. 15. In addition, 19 coordinate positions were determined as ground truth which were marked with red round markers. Position data recording is carried out at each tag placement at a ground truth position point. The total number of position estimation measurements at 19 ground truth points was 950 data.

From the recorded data, each position is then compared with the actual ground truth position and calculates the mean absolute error that occurs. This value shows the accuracy performance of TDoA positioning by using regression ranging. The results of TDoA positioning are shown with a blue triangular marker and it is shown in Fig. 16.

There are quite large deviations from the ground truth position at several points. The biggest error occurs when the tag is at the front. This can be caused by the direction of the antenna not being in the same direction and facing each other between the tag and anchor.

Fig. 13. Positioning test room area

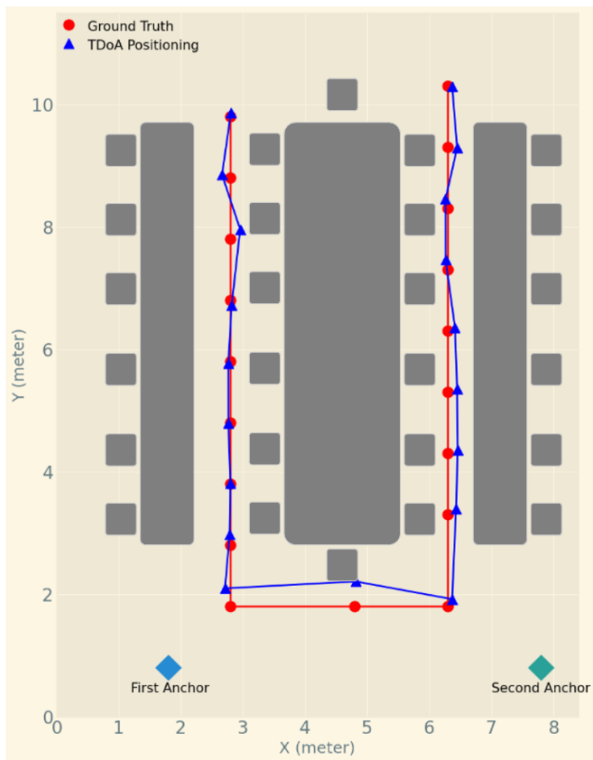Fig. 14. Installation of anchors at the front of the room


Fig. 15. Position estimation with TdoA

Fig. 16 (a) and (b) show the error analysis graph produced using the TDoA method. The position error value spreads around 0.01m to more than 1.5 m on the X-axis. Meanwhile, the error spreads around 0.01m to 1.5 m on the Y-axis.

The graph shows that there is a wide distance from the mean on both the X and Y axes, which indicates low precision. There are also outliers that reach an error above 1.5 m. This lack of precision can be caused by the number of anchors which only consists of 2 anchors, the antenna

directions not facing each other, and the presence of obstacles (furniture and wall) which can cause NLOS condition.
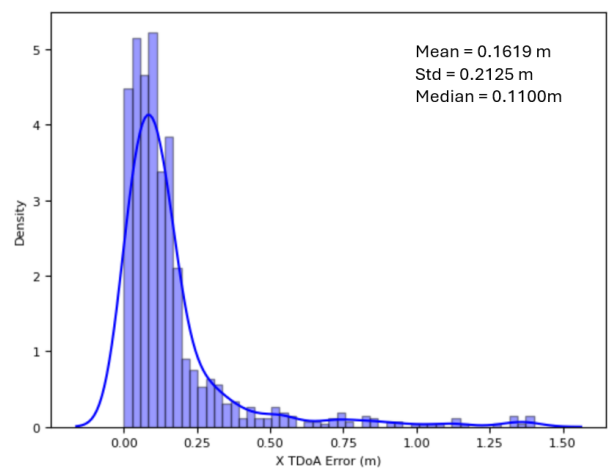
(a)
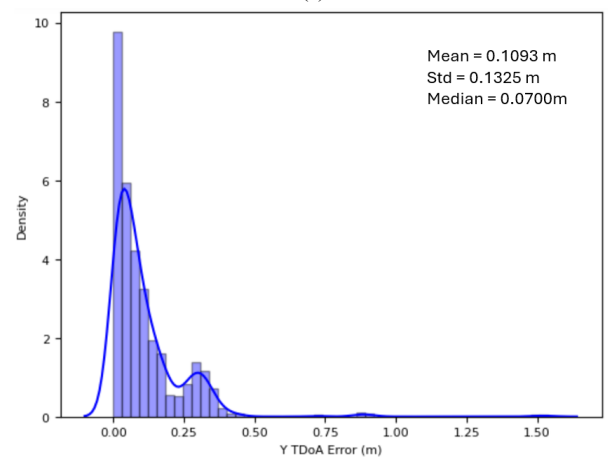
(b)

Fig. 16. Error Distribution TDoA Positioning: (a) X coordinates, (b) Y coordinates

Trilateration positioning testing uses 3 anchors [65]with anchor placement as shown in Fig. 17. Anchors 1 and 2 use the same coordinate position as TDoA positioning with an anchor distance of 6m. The coordinates of anchor 1 are (1.8m, 0.8m) and anchor 2 is at coordinates (7.8m, 0.8m). Meanwhile, the third anchor position is placed at the coordinate position (4.8m, 10.8m).
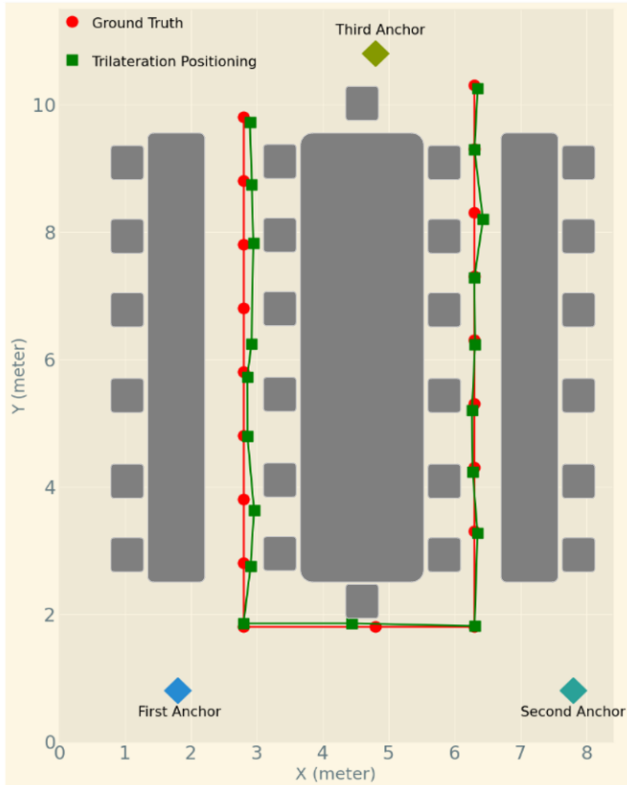

Fig. 17. Position Estimation with Trilateration

Just like TDoA positioning, in trilateration positioning 19 positions are also determined as ground truth which are marked with red round markers. The measured trilateration positioning is plotted on the green rectangular marker. In Fig. 17 it is shown that deviations occur but are still close to the position in ground truth.

When compared with TDoA, the deviation from ground truth that occurs in trilateration is smaller than with TDoA. This is due to the use of a larger number of anchors. The anchor antenna from the third anchor facing each other with the first anchor and the second anchor causes the ranging measurement to have a smaller error because the direction of the tag antenna can be accommodated by the three tags.

The trilateration positioning error distribution graph in Fig. 18(a) and Fig. 18(b) shows the error value is centered around 0.001m to greater than 1.2 m on the X-axis. Meanwhile, on the Y-axis, the error value is centered around 0.004m to 0.78m. The highest distribution value on the X axis Trilateration is quite far from the median value so it indicates low precision. The same thing happens with the Y axis Trilateration which shows the width of the error data distribution that occurs.
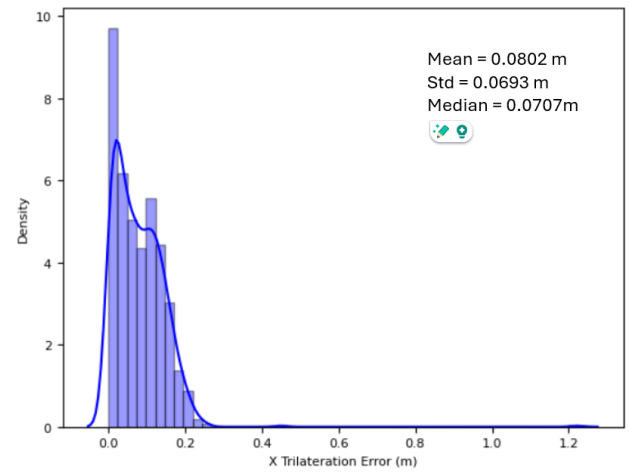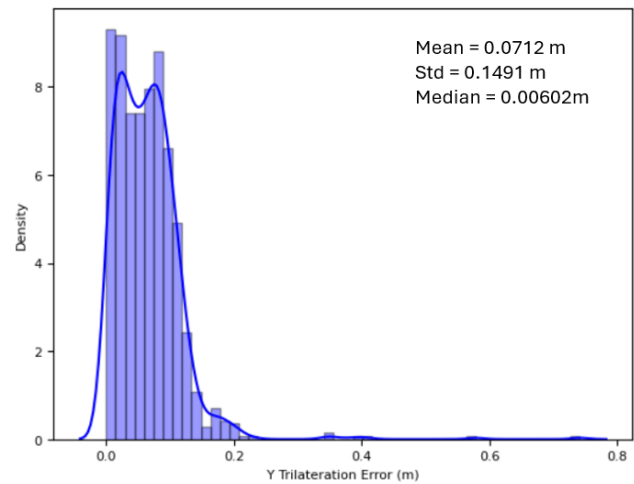
Fig. 18. Error Distribution Trilateration Positioning: (a) X coordinates, (b) Y coordinates

A comparison of precision performance between TDoA and Trilateration in Boxplot form is shown in Fig. 19. When compared with TDoA positioning, the error distribution in trilateration positioning is more convergent. This can be seen from the outliers that occur in the boxplot of the X and Y coordinates in TDoA more than in Trilateration. Apart from that, the outliers that occurred in TDoa were more spread out, reaching almost 1.6m compared to the outliers that occurred in Trilateration. This shows that the precision of trilateration positioning is better than TDoA positioning.

Trilateration Positioning provides more reliable accuracy performance. Fig. 20 shows a graph of the MAE values of the X and Y coordinates that accumulated from 19 ground truth position points for TDoA and Trilateration positioning. In TDoA positioning, an average MAE value was produced for 19 position points at X of 7.47 cm and Y of 10.49 cm. Meanwhile, the MAE of Trilateration positioning of X is 8.15 cm and Y is 8.5 cm.

The results of the implementation of positioning using TDoA and trilateration show good accuracy on the X-axis, namely producing errors in centimeter ranges. However, there is a difference in performance accuracy regarding the Y-axis. In TDoA positioning the error produced is in the

decimeter range, namely 10.49 cm, while in Trilateration positioning the error produced is in the centimeter range, namely 8.5 cm. This can be caused by the number of anchors and anchor placement. In TDoA, only 2 anchors are used which are placed on one side of the room which covers more of the X-axis area compared to the Y-axis. Meanwhile, in Trilateration there is one anchor on the other side of the room so that it can cover more of the Y-axis area. The direction of the antenna can also influence the magnitude of the error that occurred. During TDoA positioning, the direction of the Tag antenna is always towards the two antennas, whereas during Trilateration Positioning, sometimes the Tag antenna is facing away from the anchor on the other side.
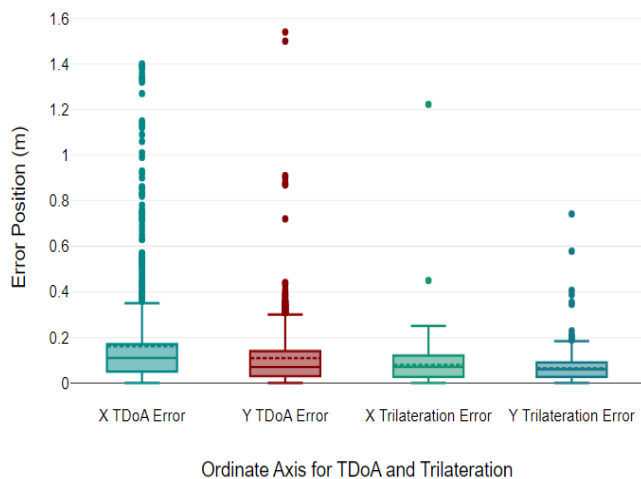

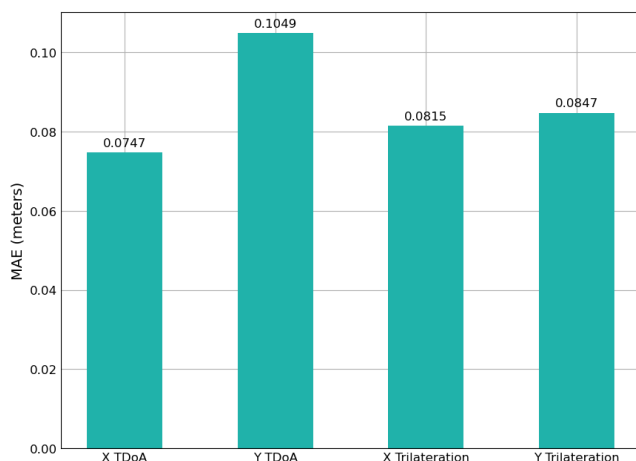Fig. 19. Error Distribution TDoa and Trilateration Box Plot

Fig. 20. MAE of TDoa and Trilateration for each ordinate

IV. CONCLUSION

Based on ranging experiments using the ESP32 UWB Pro with Display, it was found that there was a ranging error of 75.68 cm. Analysis of the ranging error data showed normality, so regression was decided as the method used to increase accuracy and succeeded in reducing the error to 5.05 cm.

Based on the resulting MAE value and the error distribution, the implementation of regression on ranging in trilateration positioning has more reliable accuracy and precision performance compared to TDoA positioning. The

MAE values that occur in Trilateration and TDoA influenced by the number of anchors, the placement of the anchors and the position of anchor and Tag Antena Positioning show that regression can be applied to positioning with accuracy in the Decimeter and Centimeter range using TDoA or Trilateration if the anchor antenna and tag are facing each other and is carried out in rooms with low obstacle complexity. However, it is still low in terms of precision due to the wide error distribution.

Experimental measurement data can be supplemented in the future with data on the direction of the tag antenna towards the anchor to accommodate the real process of NLOS indoor positioning. It is necessary to carry out more experiments in the use of ranging regression on the influence of the number of anchors, more varied anchor placement locations to obtain more complete reliability performance.

REFERENCES

[1] S. M. Asaad and H. S. Maghdid, "A Comprehensive Review of Indoor/Outdoor Localization Solutions in IoT era: Research Challenges and Future Perspectives," *Computer Networks*, vol. 212, 2022, doi: 10.1016/j.comnet.2022.109041.

[2] S. N. Ghorpade, M. Zennaro, and B. S. Chaudhari, "IoT-based hybrid optimized fuzzy threshold ELM model for localization of elderly persons," *Expert Syst. Appl.*, vol. 184, p. 115500, 2021, doi: 10.1016/j.eswa.2021.115500.

[3] R. Kanan, O. Elhassan, and R. Bensalem, "An IoT-based autonomous system for workers' safety in construction sites with real-time alarming, monitoring, and positioning strategies," *Autom. Constr.*, vol. 88, pp. 73–86, 2018, doi: 10.1016/j.autcon.2017.12.033.

[4] W. He, M. Xi, H. Gardner, B. Swift, and M. Adcock, "Spatial anchor based indoor asset tracking," in *Proceedings - 2021 IEEE Conference on Virtual Reality and 3D User Interfaces, VR 2021*, pp. 255–259, 2021, doi: 10.1109/VR50410.2021.00047.

[5] S. J. Hayward, J. Earps, R. Sharpe, K. van Lopik, J. Tribe, and A. A. West, "A novel inertial positioning update method, using passive RFID tags, for indoor asset localisation," *CIRP J. Manuf. Sci. Technol.*, vol. 35, pp. 968–982, Nov. 2021, doi: 10.1016/j.cirpj.2021.10.006.

[6] K. Staniec, M. Kowal, S. Kubal, and P. Piotrowski, "TrackMe—A Hybrid Radio-Optical System for Assets Localization in Industry 4.0 Plants," *Navigation, Journal of the Institute of Navigation*, vol. 69, no. 2, Jun. 2022, doi: 10.33012/navi.524.

[7] N. El-Sheimy and Y. Li, "Indoor navigation: state of the art and future trends," *Satellite Navigation*, vol. 2, no. 1, 2021, doi: 10.1186/s43020-021-00041-3.

[8] S. J. Hayward, K. van Lopik, C. Hinde, and A. A. West, "A Survey of Indoor Location Technologies, Techniques and Applications in Industry," *Internet of Things*, vol. 20, 2022, doi: 10.1016/j.iot.2022.100608.

[9] Y. Xianjia, L. Qingqing, J. P. Queralta, J. Heikkonen, and T. Westerlund, "Applications of UWB Networks and Positioning to Autonomous Robots and Industrial Systems," *2021 10th*

Mediterranean Conference on Embedded Computing (MECO), pp. 1-6, 2021, doi: 10.1109/MECO52532.2021.9460266.

[10] Z. Wang, S. Li, Z. Zhang, F. Lv, and Y. Hou, "Research on UWB positioning accuracy in warehouse environment," in *Procedia Computer Science*, pp. 946–951, 2018, doi: 10.1016/j.procs.2018.04.231.

[11] A. Schjørring, A. L. Cretu-Sircu, I. Rodriguez, P. Cederholm, G. Berardinelli, and P. Mogensen, "Performance Evaluation of a UWB Positioning System Applied to Static and Mobile Use Cases in Industrial Scenarios," *Electronics*, vol. 11, no. 20, Oct. 2022, doi: 10.3390/electronics11203294.

[12] K. Mascher, M. Watzko, A. Koppert, J. Eder, P. Hofer, and M. Wieser, "NIKE BLUETRACK: Blue Force Tracking in GNSS-Denied Environments Based on the Fusion of UWB, IMUs and 3D Models," *Sensors*, vol. 22, no. 8, Apr. 2022, doi: 10.3390/s22082982.

[13] X. You, D. Tian, C. Liu, X. Yu, and L. Song, "Vehicles positioning in tunnel: A real-time localization system using DL-TDOA technology," *Journal of Internet Technology*, vol. 22, no. 5, pp. 967–978, 2021, doi: 10.53106/160792642021092205003.

[14] Z. Silvia, C. Martina, S. Fabio, and P. Alessandro, "Ultra Wide Band Indoor Positioning System: analysis and testing of an IPS technology," *IFAC-PapersOnLine*, vol. 51, no. 11, pp. 1488-1492, 2018, doi: 10.1016/j.ifacol.2018.08.292.

[15] M. A. Koledoye, T. Facchinetti, and L. Almeida, "Improved MDS-based Localization with Non-line-of-sight RF Links," *Journal of Intelligent and Robotic Systems: Theory and Applications*, vol. 98, no. 1, pp. 227–237, Apr. 2020, doi: 10.1007/s10846-019-01021-1.

[16] H. K. Jeon, C. H. Lee, and Y. S. Hong, "Improvement of RTLS performance using recursive RF active echo algorithm," *Advances in Electrical and Electronic Engineering*, vol. 17, no. 2, pp. 146–154, Jun. 2019, doi: 10.15598/aeee.v17i2.3193.

[17] C. Jain, G. V. S. Sashank, N. Venkateswaran, and S. Markkandan, "Low-cost BLE based Indoor Localization using RSSI Fingerprinting and Machine Learning," in *2021 International Conference on Wireless Communications, Signal Processing and Networking, WiSPNET 2021*, pp. 363–367, 2021, doi: 10.1109/WiSPNET51692.2021.9419388.

[18] R. Ayyalasomayajula, D. Vasisht, and D. Bharadia, "BLoc: CSI-based accurate localization for BLE tags," in *CoNEXT 2018 - Proceedings of the 14th International Conference on Emerging Networking EXperiments and Technologies*, pp. 126–138, 2018, doi: 10.1145/3281411.3281428.

[19] P. Zand, J. Romme, J. Govers, F. Pasveer, and G. Dolmans, "A high-accuracy phase-based ranging solution with Bluetooth Low Energy (BLE)," in *IEEE Wireless Communications and Networking Conference, WCNC*, pp. 1-8, 2019, doi: 10.1109/WCNC.2019.8885791.

[20] J. Zhu and H. Xu, "Review of RFID-based indoor positioning technology," in *Advances in Intelligent Systems and Computing*, pp. 632–641, 2019, doi: 10.1007/978-3-319-93554-6_62.

[21] C. Duan, J. Liu, X. Ding, Z. Li, and Y. Liu, "Full-Dimension Relative Positioning for RFID-Enabled Self-Checkout Services," *Proc. ACM Interact Mob. Wearable Ubiquitous Technol.*, vol. 5, no. 1, Mar. 2021, doi: 10.1145/3448094.

[22] G. Esposito, D. Mezzogori, M. Neroni, A. Rizzi, G. Romagnoli, and M. Rosa, "A review of RFID based solutions for indoor localization and location-based classification of tags," *Proceedings of the Summer School Francesco Turco*, 2021.

[23] W. Zhang, X. Hua, K. Yu, W. Qiu, S. Zhang, and X. He, "A novel WiFi indoor positioning strategy based on weighted squared Euclidean distance and local principal gradient direction," *Sensor Review*, vol. 39, no. 1, pp. 99–106, Jan. 2019, doi: 10.1108/SR-06-2017-0109.

[24] S. Sundar, R. Kumar, and H. M. Kittur, "Improved indoor location tracking system for mobile nodes," *International Journal of Computer Aided Engineering and Technology*, vol. 12, no. 1, pp. 1-16, 2020.

[25] J. Przewocki, M. J. Ammann, and A. Narbudowicz, "Measurement of Orientation and Distance Change Using Circularly Polarized UWB Signals," *IEEE Trans. Antennas Propag.*, vol. 70, no. 6, pp. 4803–4809, Jun. 2022, doi: 10.1109/TAP.2022.3140500.

[26] J. Bauwens, N. Macoir, S. Giannoulis, I. Moerman, and E. De Poorter, "UWB-MAC: MAC protocol for UWB localization using ultra-low power anchor nodes," *Ad Hoc Networks*, vol. 123, Dec. 2021, doi: 10.1016/j.adhoc.2021.102637.

[27] R. Vleugels, B. Van Herbruggen, J. Fontaine, and E. De Poorter, "Ultra-wideband indoor positioning and imu-based activity recognition for ice hockey analytics," *Sensors*, vol. 21, no. 14, Jul. 2021, doi: 10.3390/s21144650.

[28] A. Benini, A. Mancini, and S. Longhi, "An IMU/UWB/vision-based extended kalman filter for mini-UAV localization in indoor environment using 802.15.4a wireless sensor network," *Journal of Intelligent and Robotic Systems: Theory and Applications*, vol. 70, no. 1–4, pp. 461–476, Apr. 2013, doi: 10.1007/s10846-012-9742-1.

[29] E. Shahid, Q. Arain, S. Kumari, and I. Farah, "Images based indoor positioning using AI and crowdsourcing," in *ACM International Conference Proceeding Series*, pp. 97–101, 2019, doi: 10.1145/3318396.3318415.

[30] Y. Wei and B. Akinci, "End-to-end Image-based Indoor Localization for Facility Operation and Management," *ISARC. Proceedings of the International Symposium on Automation and Robotics in Construction*, vol. 35, pp. 1-9, 2018.

[31] Y. Wu, X. Liu, W. Guan, B. Chen, X. Chen, and C. Xie, "High-speed 3D indoor localization system based on visible light communication using differential evolution algorithm," *Opt. Commun.*, vol. 424, pp. 177–189, 2018, doi: 10.1016/j.optcom.2018.04.062.

[32] S. Li and R. Rashidzadeh, "A Hybrid Indoor Location Positioning System," *2018 IEEE International Conference on Electro/Information Technology (EIT)*, pp. 0187-0191, 2018, doi: 10.1109/EIT.2018.8500265.

[33] Q. Shi, S. Zhao, X. Cui, M. Lu, and M. Jia, "Anchor self-localization algorithm based on UWB ranging and inertial measurements," in *Tsinghua Science and Technology*, vol. 24, no. 6, pp. 728-737, Dec. 2019, doi: 10.26599/TST.2018.9010102.

[34] G. I. Hapsari, R. Munadi, B. Erfianto, and I. D. Irawati, "Research Trend Topic Area on Mobile Anchor Localization: A Systematic Mapping Study," *International journal of electrical and computer engineering systems*, vol. 14, no. 9, pp. 959-972, 2023.

[35] J. Kunhoth, A. G. Karkar, S. Al-Maadeed, and A. Al-Ali, "Indoor positioning and wayfinding systems: a survey," *Human-centric Computing and Information Sciences*, vol. 10, no. 1, 2020, doi: 10.1186/s13673-020-00222-0.

[36] N. C. Syazwani, N. H. A. Wahab, N. Sunar, S. H. Ariffin, K. Y. Wong, and Y. Aun, "Indoor positioning system: A review," *International Journal of Advanced Computer Science and Applications*, vol. 13, no. 6, 2022.

[37] X. Gao, H. R. Sadjadpour, F. U. Dowla and F. Nekoogar, "Optimal Communication System With Power Control and Ultra-Wideband Propagation Channel Model Designs for Monitoring Harsh Through-Wall Environments," in *IEEE Access*, vol. 12, pp. 56226-56239, 2024, doi: 10.1109/ACCESS.2024.3389681.

[38] J. Ninnemann, P. Schwarzbach, and O. Michler, "Toward UWB Impulse Radio Sensing: Fundamentals, Potentials, and Challenges," in *UWB Technology - New Insights and Developments*, 2023, doi: 10.5772/intechopen.110040.

[39] F. Zafari, A. Gkelias, and K. K. Leung, "A Survey of Indoor Localization Systems and Technologies," *IEEE Communications Surveys and Tutorials*, vol. 21, no. 3, pp. 2568–2599, 2019, doi: 10.1109/COMST.2019.2911558.

[40] M. Ridolfi, A. Kaya, R. Berkvens, M. Weyn, W. Joseph, and E. De Poorter, "Self-calibration and collaborative localization for uwb positioning systems: A survey and future research directions," *ACM Computing Surveys*, vol. 54, no. 4, 2021, doi: 10.1145/3448303.

[41] N. Smaoui, M. Heydariaan, and O. Gnawali, "Anchor-oriented Time and Phase-based Concurrent Self-localization using UWB Radios," *2021 IEEE 46th Conference on Local Computer Networks (LCN)*, pp. 265-272, 2021, doi: 10.1109/LCN52139.2021.9524990.

[42] S. Chen, Z. Shi, F. Wu, C. Wang, J. Liu, and J. Chen, "Improved 3-D indoor positioning based on particle swarm optimization and the Chan method," *Information*, vol. 9, no. 9, Aug. 2018, doi: 10.3390/info9090208.

[43] C. L. Sang, M. Adams, T. Hörmann, M. Hesse, M. Porrmann, and U. Rückert, "An Analytical Study of Time of Flight Error Estimation in Two-Way Ranging Methods," *2018 International Conference on*

Indoor Positioning and Indoor Navigation (IPIN), pp. 1-8, 2018, doi: 10.1109/IPIN.2018.8533697.

[44] C. L. Sang, M. Adams, T. Hörmann, M. Hesse, M. Porrmann, and U. Rückert, "Numerical and experimental evaluation of error estimation for two-way ranging methods," *Sensors*, vol. 19, no. 3, p. 616, 2019.

[45] C. L. Sang, M. Adams, T. Hörmann, M. Hesse, M. Porrmann, and U. Rückert, "Numerical and Experimental Evaluation of Error Estimation for Two-Way Ranging Methods," *Methods*, pp. 24–27, 2018, doi: 10.4119/unibi/2919795.

[46] M. M. Din, N. Jamil, J. Maniam, and M. A. Mohamed, "Review of indoor localization techniques," *International Journal of Engineering & Technology*, vol. 7, no. 2, pp. 201-204, 2018.

[47] I. D. Sumitra, S. Supatmi, and R. Hou, "Enhancement of Indoor Localization Algorithms in Wireless Sensor Networks: A Survey," in *IOP Conference Series: Materials Science and Engineering*, vol. 407, no. 1, p. 012068, 2018, doi: 10.1088/1757-899X/407/1/012068.

[48] L. Flueratoru, S. Wehrli, M. Magno, E. S. Lohan, and D. Niculescu, "High-Accuracy Ranging and Localization With Ultrawideband Communications for Energy-Constrained Devices," in *IEEE Internet of Things Journal*, vol. 9, no. 10, pp. 7463-7480, 15 May15, 2022, doi: 10.1109/JIOT.2021.3125256.

[49] V. V Krzhizhanovskaya, · Jack, J. Dongarra, · Peter, and M. A. Sloot, "Static and Dynamic Comparison of Pozyx and DecaWave UWB Indoor Localization Systems with Possible Improvements book," in *Maciej Paszynski · Dieter Kranzlmüller · Computational Science-ICCS 2021*, 2021.

[50] T. Polonelli, S. Schläpfer, and D. ETH Zurich Zurich, "Performance Comparison between Decawave DW1000 and DW3000 in low-power double side ranging applications," in *Conference Paper Funding acknowledgement: 187087-AeroSense: a novel MEMS-based surface pressure and acoustic IoT measurement system for wind turbines (SNF)*, 2022.

[51] A. R. Jiménez and F. Seco, "Improving the accuracy of decawave's uwb mdek1001 location system by gaining access to multiple ranges," *Sensors*, vol. 21, no. 5, pp. 1–31, Mar. 2021, doi: 10.3390/s21051787.

[52] J. Sidorenko, V. Schatz, N. Scherer-Negenborn, M. Arens, and U. Hugentobler, "Error Corrections for Ultrawideband Ranging," *IEEE Trans. Instrum. Meas.*, vol. 69, no. 11, pp. 9037–9047, Nov. 2020, doi: 10.1109/TIM.2020.2996706.

[53] V. Barral Vales, O. C. Fernández, T. Domínguez-Bolaño, C. J. Escudero, and J. A. García-Naya, "Fine Time Measurement for the Internet of Things: A Practical Approach Using ESP32," in *IEEE Internet of Things Journal*, vol. 9, no. 19, pp. 18305-18318, 1 Oct.1, 2022, doi: 10.1109/JIOT.2022.3158701.

[54] F. Despaux, A. van den Bossche, K. Jaffrès-Runser, and T. Val, "N-TWR: An accurate time-of-flight-based N-ary ranging protocol for Ultra-Wide band," *Ad Hoc Networks*, vol. 79, pp. 1–19, 2018, doi: 10.1016/j.adhoc.2018.05.016.

[55] F. Tian and H. Li, "Study on the improved unscented Kalman filter ultra-wideband indoor location algorithm based on two-way time-of-flight," *Journal of Engineering Science and Technology Review*, vol. 11, no. 5, pp. 93–99, 2018, doi: 10.25103/jestr.115.11.

[56] B. V. Herbruggen, S. Luchie, R. Berkvens, J. Fontaine and E. D. Poorter, "Impact of CIR processing for UWB radar distance estimation with the DW1000 transceiver," *2023 13th International Conference on Indoor Positioning and Indoor Navigation (IPIN)*, pp. 1-7, 2023, doi: 10.1109/IPIN57070.2023.10332499.

[57] G. Hollosi, C. Lukovszki, and M. Bancsics, "Radio Resource Efficient UWB Measurement System Design and Performance Analysis for TWR-based Ranging," in *Proceedings - 2022 IEEE 5th International Conference on Industrial Cyber-Physical Systems, ICPS 2022*, 2022, doi: 10.1109/ICPS51978.2022.9816970.

[58] W. Wang, J. Huang, S. Cai, and J. Yang, "Design and implementation of synchronization-free TDOA localization system based on UWB," *Radioengineering*, vol. 28, no. 1, pp. 320–330, Apr. 2019, doi: 10.13164/re.2019.0320.

[59] V. Navratil, J. Krska, and F. Vejrazka, "Concurrent Bidirectional TDoA Positioning in UWB Network with Free-Running Clocks," *IEEE Trans. Aerosp. Electron. Syst.*, vol. 58, no. 5, pp. 4434–4450, Oct. 2022, doi: 10.1109/TAES.2022.3161895.

[60] E. Weine, M. S. McPeek, and M. Abney, "Application of Equal Local Levels to Improve Q-Q Plot Testing Bands with R Package qqconf," *J. Stat. Softw.*, vol. 106, 2023, doi: 10.18637/jss.v106.i10.

[61] M. Martalo, G. Ferrari, S. Perri, G. Verdano, F. De Mola, and F. Monica, "UWB TDoA-based Positioning Using a Single Hotspot with Multiple Anchors," in *2019 4th International Conference on Computing, Communications and Security, ICCCS 2019*, 2019, doi: 10.1109/CCCS.2019.8888099.

[62] J. Tiemann and C. Wietfeld, "Scalable and Precise Multi-UAV Indoor Navigation using TDOA-based UWB Localization," in *2017 International Conference on Indoor Positioning and Indoor Navigation (IPIN)*, 2017.

[63] B. Choi, K. La, and S. Lee, "UWB TDOA/TOA measurement system with wireless time synchronization and simultaneous tag and anchor positioning," *2018 IEEE International Conference on Computational Intelligence and Virtual Environments for Measurement Systems and Applications (CIVEMSA)*, pp. 1-6, 2018, doi: 10.1109/CIVEMSA.2018.8439949.

[64] J. J. Pérez-Solano, S. Ezpeleta, and J. M. Claver, "Indoor localization using time difference of arrival with UWB signals and unsynchronized devices," *Ad Hoc Networks*, vol. 99, Mar. 2020, doi: 10.1016/j.adhoc.2019.102067.

[65] J. Luomala and I. Hakala, "Adaptive range-based localization algorithm based on trilateration and reference node selection for outdoor wireless sensor networks," *Computer Networks*, vol. 210, p. 108865, 2022, doi: 10.1016/j.comnet.2022.108865.